

ERRATUM: “A SECOND CASE OF VARIABLE Na I D LINES IN A HIGHLY-REDDENED TYPE Ia SUPERNOVA” (2009, ApJ, 693, 207)

STÉPHANE BLONDIN,^{1,2,*} JOSÉ L. PRIETO,^{3,†} FERDINANDO PATAT,² PETER CHALLIS,¹ MALCOLM HICKEN,¹ ROBERT P. KIRSHNER,^{1,‡} THOMAS MATHESON,⁴ MARYAM MODJAZZ^{5,§}

1. NO VARIABLE Na I D LINES IN SN 1999cl

The large variation in the Na I D equivalent width (EW) observed in the Type Ia SN 1999cl (Blondin et al. 2009), $\Delta\text{EW} = 1.66 \pm 0.21 \text{ \AA}$, results in fact from a measurement error. The origin of this error was traced back to observed wavelength shifts of the Na I D profile with respect to its expected restframe location (5889.95 and 5895.92 \AA for the D₂ and D₁ lines, respectively), which were not properly taken into account in a revised implementation of our EW computation (albeit correctly displayed on the graphical interface developed for these measurements; see Fig. 1). We revised *all* the measurements in the original paper, and can confirm that SN 1999cl is the only object of our sample affected by this error (see Fig. 2). In particular, measurements for SN 2006X are not affected when properly taking into account these wavelength shifts (see open squares in Fig. 2). Since our measurement routines were validated based on SN 2006X, for which high-resolution VLT+UVES data were available (Patat et al. 2007), and for which our own EW determinations on lower-resolution FLWO 1.5 m+FAST data yielded consistent results, this error went unnoticed.

SN 1999cl displays the largest wavelength shifts of the Na I D profile of all the SNe Ia in our sample, with typical shifts of approximately -6 \AA , corresponding to a $\sim 300 \text{ km s}^{-1}$ velocity blueshift with respect to its expected restframe location. This velocity shift corresponds to the difference between the recession velocity of the host-galaxy nucleus (2338 km s^{-1} for NGC 4501; Falco et al. 1999), which we used to de-redshift the SN 1999cl spectra, and that derived at the location of SN 1999cl from emission lines in the SN spectrum used for classification purposes by Garnavich et al. (1999), namely $cz = 2030 \text{ km s}^{-1}$. It results from the location

of SN 1999cl in a spiral arm with a blueshifted velocity along the line of sight, as derived from kinematic maps of NGC 4501 based on H I emission by Chemin et al. (2006). We note that Garnavich et al. (1999) had in fact correctly reported a Na I D EW of 0.33 nm for their first spectrum of SN 1999cl, consistent with our revised measurement on the same spectrum.

All the other objects in our sample display significantly lower wavelength shifts of the Na I D profile ($\lesssim 4 \text{ \AA}$ in absolute value; see Fig. 2). We have not investigated the exact nature of the observed wavelength shifts for all the objects in our sample, but simply note that absolute shifts at the $\lesssim 4 \text{ \AA}$ level do not appear to affect our revised EW measurements, with an RMS difference compared to our original measurements of only $\sim 0.13 \text{ \AA}$.

Our new measurements show that the EW variation for the Na I D profile in SN 1999cl is significantly lower than reported in our original paper ($0.43 \pm 0.14 \text{ \AA}$ cf. $1.66 \pm 0.21 \text{ \AA}$). While the EW variation remains statistically significant (3.1σ different from zero), it is now below the detection threshold of 0.5 \AA derived from the Monte Carlo simulations published in the original paper (these simulations are unaffected by the aforementioned measurement error). We also note that the S/N cut based on these same MC simulations ($S/N \geq 50$ per pixel) was erroneously applied based on the \bar{S}/N per \AA instead of per dispersion element (typically $\sim 1.5 \text{ \AA}$ per pixel), resulting in the exclusion of spectra with $50 \leq S/N \text{ per pixel} \leq 50 \times 1.5 = 75$. Our revised measurements thus typically include more spectra for a given SN than in the original paper (see Table 1).

As a result, SN 1999cl should no longer be considered as an object displaying variable Na I D lines in our study. The fraction of SNe Ia in our sample displaying Na I D lines thus goes from $\sim 6\%$ (2/31) in the original study to $\sim 3\%$ (1/31) in the revised analysis, SN 2006X being the only SN Ia in our sample with variable Na I D lines.

The main conclusion of our paper remains unchanged. Quoting from the conclusions section in the original paper: “We conclude that either variable Na I D features are not a common property of SNe Ia, or that the level of the variation is less on average than observed in SN 2006X.” However, the title of our paper highlighted the new detection of “variable Na I D lines in a highly-reddened Type Ia supernova” (i.e., SN 1999cl), which no longer holds.

Our revised measurements affect Figs. 3, 4, and 5 of the original paper, as well as Table 2. We present revised versions of these in what follows (Figs. 4, 5, 6, and Table 1). In addition, we noticed a small error in the legend labels of Fig. 2 in the original paper, which is corrected

¹ Harvard-Smithsonian Center for Astrophysics, 60 Garden Street, Cambridge, MA 02138

² European Southern Observatory, Karl-Schwarzschild-Strasse 2, D-85748 Garching, Germany

³ Dept. of Astronomy, The Ohio State University, 140 W. 18th Ave., Columbus, OH 43210

⁴ National Optical Astronomy Observatory, 950 North Cherry Avenue, Tucson, AZ 85719-4933

⁵ Department of Astronomy, University of California, Berkeley, CA 94720-3411

* Now at: Aix Marseille Univ, CNRS, LAM, Laboratoire d’Astrophysique de Marseille, Marseille, France

† Now at: Núcleo de Astronomía de la Facultad de Ingeniería, Universidad Diego Portales, Av. Ejército 441, Santiago, Chile; Millennium Institute of Astrophysics, Santiago, Chile

‡ Now also at: Gordon and Betty Moore Foundation, 1661 Page Mill Road, Palo Alto, CA 94304, USA

§ Now at: Center for Cosmology and Particle Physics, New York University, 4 Washington Place, New York, NY 10003, USA

in the new Fig. 3 below.

We are indebted to Lingzhi Wang, currently a research scholar at the Chinese Academy of Sciences South Amer-

ica Center for Astronomy in Santiago, Chile, for having brought this measurement error to our attention during the conference “Supernovae through the ages” held on Easter Island, Chile, during August 2016.

REFERENCES

- Barbon, R., Benetti, S., Rosino, L., Cappellaro, E., & Turatto, M. 1990, *A&A*, 237, 79
- Blondin, S., Prieto, J. L., Patat, F., et al. 2009, *ApJ*, 693, 207
- Chemin, L., Balkowski, C., Cayatte, V., et al. 2006, *MNRAS*, 366, 812
- Falco, E. E., Kurtz, M. J., Geller, M. J., et al. 1999, *PASP*, 111, 438
- Garnavich, P., Jha, S., Kirshner, R., Challis, P., & Szentgyorgyi, A. 1999, *IAU Circ.*, 7198
- Jha, S., Riess, A. G., & Kirshner, R. P. 2007, *ApJ*, 659, 122
- Patat, F., Chandra, P., Chevalier, R., et al. 2007, *Science*, 317, 924
- Turatto, M., Benetti, S., & Cappellaro, E. 2003, in *From Twilight to Highlight: The Physics of Supernovae*, ed. W. Hillebrandt & B. Leibundgut, 200–+

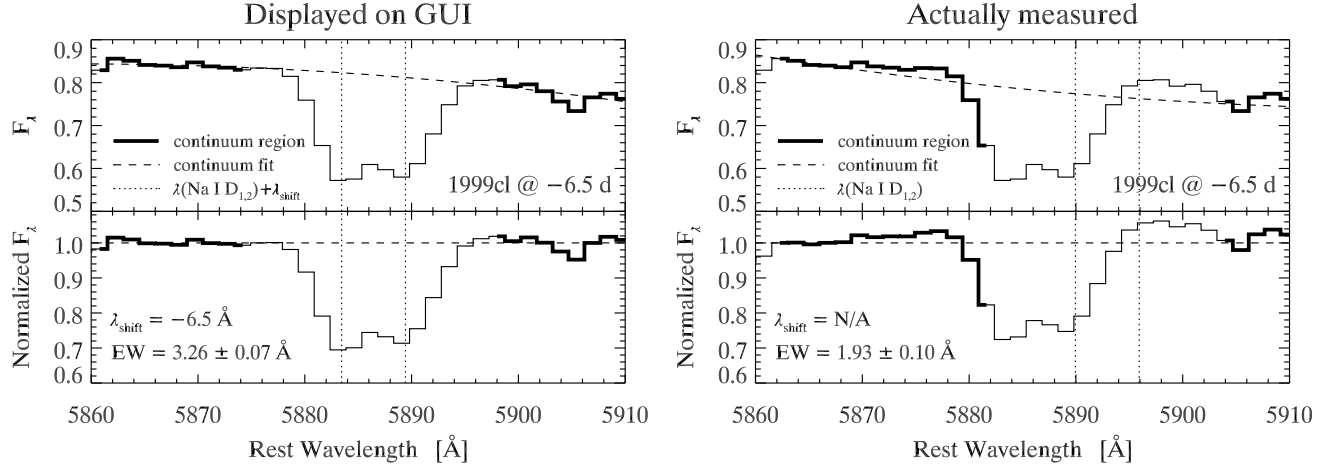


FIG. 1.— Impact of the observed wavelength shift of the Na I D profile on the EW measurement, illustrated using the SN 1999cl spectrum at -6.5 d from maximum light. The left panel reproduces what was displayed on the graphical interface used to determine the continuum-fit regions on either side of the Na I D profile (thick black lines), with the rest-wavelength locations of the D₂ and D₁ lines shifted by $\lambda_{\text{shift}} = -6.5$ Å (dotted lines) with respect to their true locations (5889.95 and 5895.92 Å, respectively). Division by the continuum fit (dashed line) yields a normalized profile (lower panel) appropriate for computing the profile EW, here determined to be 3.26 ± 0.07 Å. However, in our revised implementation of the EW computation the wavelength ranges of the continuum-fit regions were passed to a separate function where the wavelength shift was accidentally ignored (i.e., $\lambda_{\text{shift}} = 0$). Since the continuum wavelength ranges were determined with respect to the rest-wavelength locations of the D₂ and D₁ lines, this resulted in an erroneous continuum fit and subsequent underestimate of the true EW (1.93 ± 0.10 Å instead of 3.26 ± 0.07 Å). SN 1999cl is the only object affected by this analysis error, which thus went unnoticed in our various validation tests based on SN 2006X.

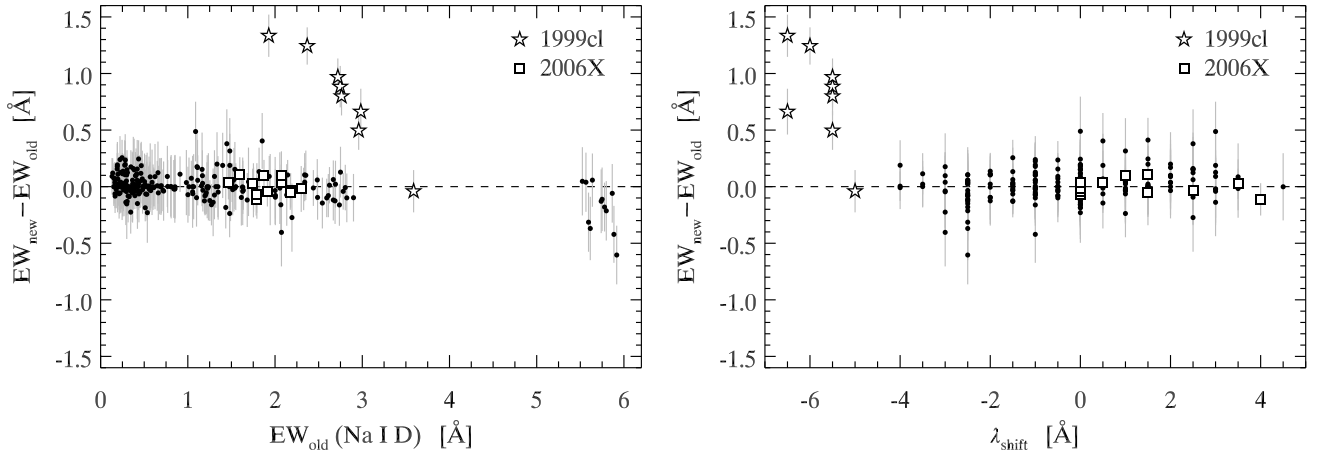


FIG. 2.— *Left*: Difference between our revised (EW_{new}) and original (EW_{old}) Na I D EW measurements *vs.* our original measurements. Only SN 1999cl is systematically and largely affected (open stars), with typical differences in excess of 0.5 Å at the 3σ level. Excluding SN 1999cl, the RMS of all other residuals is only ~ 0.13 Å. The RMS residual for SN 2006X is even lower, at ~ 0.07 Å (open squares). *Right*: Difference between our revised and original Na I D EW measurements *vs.* the measured wavelength shift of the Na I D profile (λ_{shift}), manually adjusted in 0.5 Å steps. Only SN 1999cl (open stars) displays absolute shifts at the $\gtrsim 5$ Å level, while measurements corresponding to $|\lambda_{\text{shift}}| \lesssim 4$ Å are not significantly affected (including SN 2006X, open squares).

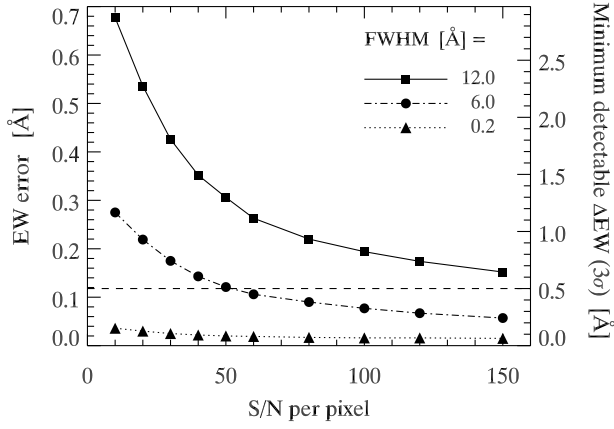


FIG. 3.— [Figure 2 in Blondin et al. (2009)]. EW measurement error as a function of S/N for three FWHM resolutions. The dash-dotted curve corresponds to the resolution of our data set (FWHM ≈ 6 Å). The ordinate axis on the right indicates the corresponding 3σ error on the difference between EW measurements. The horizontal dashed line corresponds to a minimum detectable EW difference of 0.5 Å.

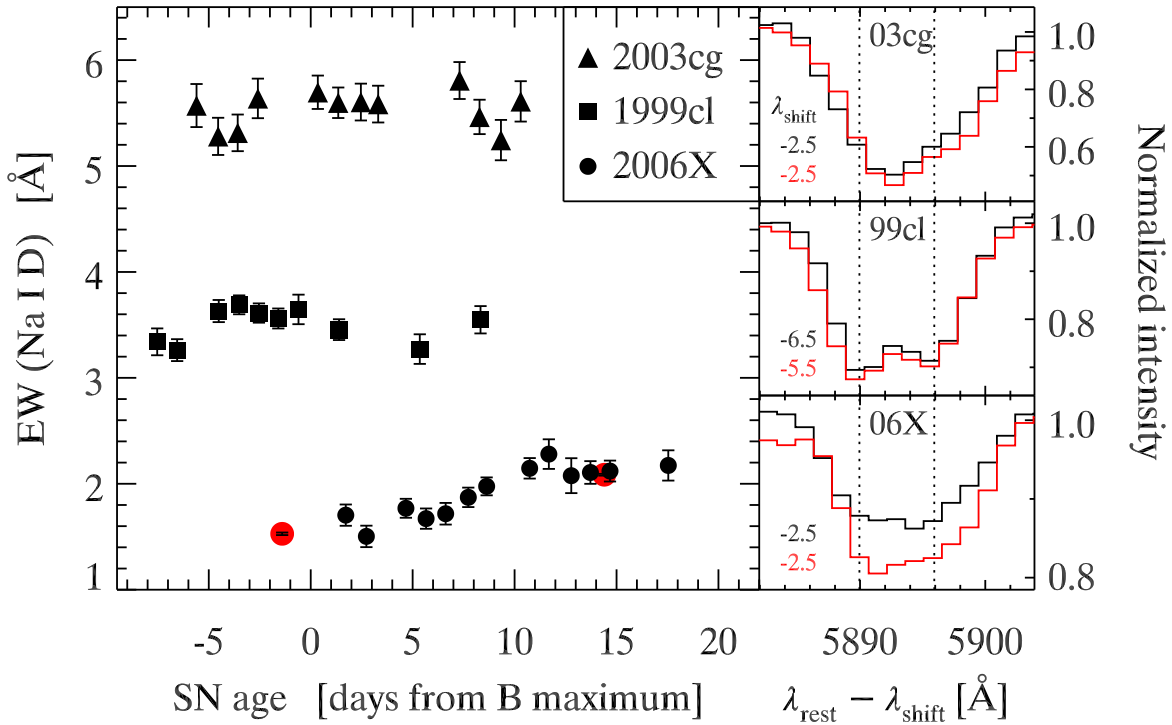


FIG. 4.— [Figure 3 in Blondin et al. (2009)]. Left: Time-evolution of the equivalent width of the NaID doublet for the three most highly-reddened SNe Ia in our sample: SNe 2003cg (filled triangles), 1999cl (filled squares), and 2006X (filled circles). Only SN 2006X exhibits clear variable NaID EWs, while those of SN 1999cl and SN 2003cg remain largely constant over time. The larger filled circles at -2 d and $+14$ d correspond to EW measurements on high-resolution (FWHM ≈ 7 km s $^{-1}$, or ~ 0.14 Å, at NaID) VLT+UVES spectra of SN 2006X published by Patat et al. (2007). Right: Normalized NaID profiles for SN 2003cg (top), SN 1999cl (middle) and SN 2006X (bottom), plotted in rest-frame wavelength corrected for the shift in wavelength of the NaID doublet, λ_{shift} , whose value is indicated for each profile. The black and red lines correspond to the smallest and largest EW, respectively. Note the difference in ordinate range, decreasing from top to bottom. The vertical dotted lines indicate the wavelength positions of the individual D₂ and D₁ lines. [See the electronic version of the Journal for a color version of this figure.]

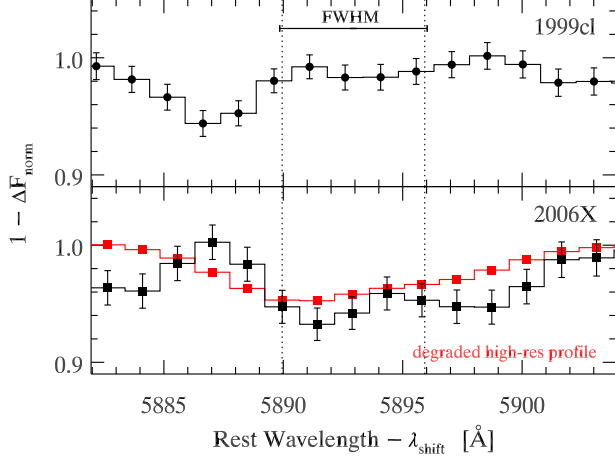


FIG. 5.— [Figure 4 in Blondin et al. (2009)]. One minus the difference between the normalized Na I D profiles with the smallest and largest EW, respectively, for SN 1999cl (top) and SN 2006X (bottom). The wavelengths have been corrected for the shift in wavelength of the Na I D doublet, λ_{shift} (see Fig. 4). The red line in the lower panel corresponds to the variation for SN 2006X inferred by degrading the resolution of the high-resolution spectra published by Patat et al. (2007). The vertical dotted lines indicate the rest wavelength positions of the individual D₂ and D₁ lines. The horizontal line in the upper panel shows the size of one spectral resolution element (FWHM ≈ 6 Å). [See the electronic version of the Journal for a color version of this figure.]

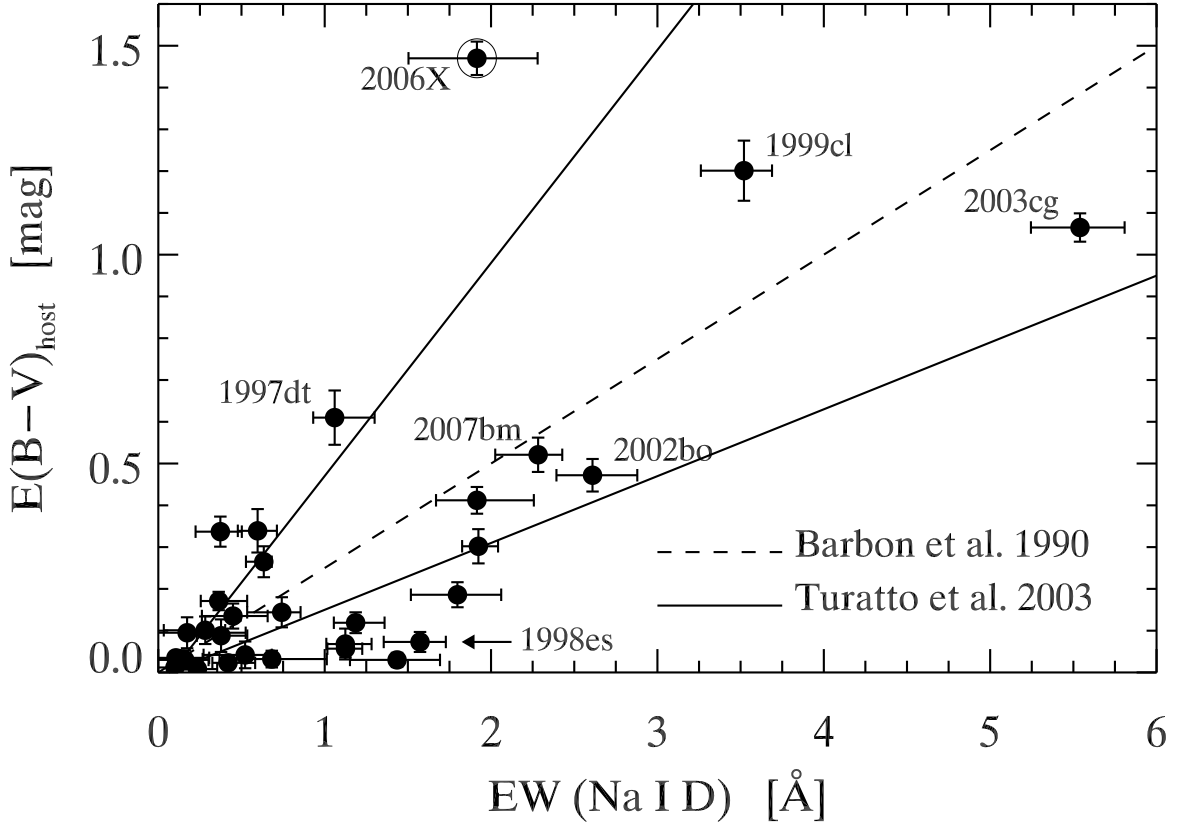


FIG. 6.— [Figure 5 in Blondin et al. (2009)]. Host-galaxy color excess versus equivalent width of the Na I D doublet for the 31 SNe Ia in our sample. The error bar for EW(Na I D) corresponds to the full range of the observed variation. Also shown are the empirical relations of Barbon et al. (1990) and Turatto et al. (2003), also derived using SN Ia data.

TABLE 1
[Table 2 in Blondin et al. (2009)]. REDDENING AND NAID EW
 MEASUREMENTS

| SN | $E(B - V)$ | EW | ΔEW | N_σ | χ^2_ν | dof | t_{\min} | Δt |
|--------|-------------|------------------------|-------------------|------------|--------------|-----|------------|------------|
| (1) | (mag) | (Å) | (Å) | (5) | (const.) | (7) | (d) | (d) |
| 1994D | 0.04 (0.01) | $0.11^{+0.20}_{-0.20}$ | 0.40 (0.24) | 1.6 | 2.10 | 13 | -9.5 | 59.6 |
| 1994ae | 0.02 (0.01) | $0.42^{+0.16}_{-0.09}$ | 0.26 (0.18) | 1.4 | 0.68 | 10 | +1.4 | 38.6 |
| 1995al | 0.06 (0.02) | $1.12^{+0.10}_{-0.11}$ | 0.21 (0.21) | 1.0 | 0.84 | 8 | +7.0 | 61.5 |
| 1997bp | 0.19 (0.03) | $1.80^{+0.26}_{-0.28}$ | 0.54 (0.23) | 2.3 | 1.53 | 7 | -1.1 | 28.6 |
| 1997br | 0.27 (0.04) | $0.63^{+0.05}_{-0.11}$ | 0.15 (0.24) | 0.6 | 0.25 | 4 | -7.4 | 28.7 |
| 1997do | 0.10 (0.03) | $0.28^{+0.12}_{-0.25}$ | 0.37 (0.21) | 1.8 | 0.61 | 8 | -6.1 | 27.5 |
| 1997dt | 0.61 (0.07) | $1.06^{+0.24}_{-0.13}$ | 0.37 (0.24) | 1.6 | 1.02 | 3 | -7.9 | 8.9 |
| 1998aq | 0.01 (0.01) | $0.23^{+0.12}_{-0.16}$ | 0.28 (0.18) | 1.5 | 0.60 | 20 | -9.0 | 87.6 |
| 1998bu | 0.34 (0.04) | $0.37^{+0.13}_{-0.15}$ | 0.28 (0.16) | 1.7 | 0.62 | 26 | -2.7 | 59.8 |
| 1998dh | 0.17 (0.02) | $0.36^{+0.17}_{-0.11}$ | 0.28 (0.28) | 1.0 | 0.29 | 4 | -8.8 | 8.8 |
| 1998dm | 0.34 (0.05) | $0.60^{+0.12}_{-0.12}$ | 0.23 (0.27) | 0.9 | 0.22 | 5 | +5.8 | 18.9 |
| 1998es | 0.07 (0.02) | $1.57^{+0.15}_{-0.22}$ | 0.37 (0.24) | 1.6 | 0.36 | 15 | -6.0 | 36.4 |
| 1999cl | 1.20 (0.07) | $3.52^{+0.17}_{-0.26}$ | 0.43 (0.14) | 3.1 | 2.07 | 9 | -7.5 | 15.8 |
| 1999dq | 0.12 (0.03) | $1.19^{+0.17}_{-0.13}$ | 0.30 (0.22) | 1.4 | 0.45 | 15 | -9.6 | 39.3 |
| 2001V | 0.03 (0.02) | $1.44^{+0.26}_{-0.28}$ | 0.54 (0.28) | 2.0 | 0.72 | 14 | -9.3 | 33.4 |
| 2001en | 0.07 (0.04) | $1.12^{+0.16}_{-0.11}$ | 0.27 (0.31) | 0.9 | 0.35 | 4 | +2.7 | 8.7 |
| 2001ep | 0.14 (0.04) | $0.74^{+0.11}_{-0.21}$ | 0.32 (0.27) | 1.2 | 0.36 | 10 | -2.7 | 10.8 |
| 2002bo | 0.47 (0.04) | $2.61^{+0.27}_{-0.22}$ | 0.49 (0.20) | 2.4 | 1.09 | 21 | -7.0 | 36.7 |
| 2002cr | 0.09 (0.04) | $0.38^{+0.16}_{-0.15}$ | 0.30 (0.22) | 1.4 | 0.48 | 4 | -7.4 | 12.8 |
| 2002fk | 0.03 (0.02) | $0.12^{+0.14}_{-0.13}$ | 0.28 (0.23) | 1.2 | 0.87 | 7 | -0.6 | 31.6 |
| 2003cg | 1.06 (0.03) | $5.54^{+0.27}_{-0.29}$ | 0.56 (0.26) | 2.2 | 0.97 | 11 | -5.6 | 15.9 |
| 2003du | 0.01 (0.01) | $0.10^{+0.17}_{-0.22}$ | 0.39 (0.22) | 1.8 | 0.77 | 12 | -9.7 | 38.8 |
| 2003kf | 0.04 (0.03) | $0.52^{+0.16}_{-0.25}$ | 0.41 (0.20) | 2.0 | 0.38 | 14 | -7.3 | 48.4 |
| 2005am | 0.03 (0.02) | $0.16^{+0.14}_{-0.22}$ | 0.37 (0.21) | 1.7 | 0.60 | 7 | +0.4 | 8.9 |
| 2005cf | 0.10 (0.04) | $0.17^{+0.35}_{-0.18}$ | 0.53 (0.28) | 1.9 | 1.03 | 23 | -11.8 | 41.7 |
| 2006N | 0.03 (0.02) | $0.68^{+0.33}_{-0.31}$ | 0.65 (0.28) | 2.3 | 1.21 | 7 | -2.8 | 11.8 |
| 2006X | 1.47 (0.04) | $1.92^{+0.36}_{-0.41}$ | 0.78 (0.17) | 4.5 | 3.68 | 18 | +1.7 | 58.5 |
| 2007S | 0.41 (0.03) | $1.92^{+0.34}_{-0.25}$ | 0.59 (0.25) | 2.3 | 1.20 | 6 | -4.7 | 29.6 |
| 2007af | 0.14 (0.03) | $0.45^{+0.21}_{-0.19}$ | 0.40 (0.20) | 1.9 | 0.86 | 24 | -4.7 | 97.2 |
| 2007bm | 0.52 (0.04) | $2.28^{+0.14}_{-0.26}$ | 0.40 (0.16) | 2.5 | 1.34 | 6 | -9.3 | 29.8 |
| 2007ca | 0.30 (0.04) | $1.92^{+0.12}_{-0.10}$ | 0.22 (0.31) | 0.7 | 0.16 | 3 | +3.4 | 9.9 |

NOTE. — Col. (1): SN name; col. (2): host-galaxy color excess determined from fits to multi-band optical light curves using the MLCS2k2 code of Jha et al. (2007); col. (3): weighted mean EW. The upper and lower limits correspond to the maximum deviations from the weighted mean; col. (4): maximum EW difference. The 1σ error appears in between parentheses; col. (5): ΔEW divided by its 1σ error; col. (6): χ^2 per degree of freedom for a constant EW fit; col. (7): number of degrees of freedom (simply the number of data points minus one); col. (8): age (in days from B -band maximum light) of the earliest spectrum; col. (9): age range (in days) of the spectra used in the fit.

A SECOND CASE OF VARIABLE Na I D LINES IN A HIGHLY-REDDENED TYPE Ia SUPERNOVA

S. BLONDIN,^{1,2} J. L. PRIETO,³ F. PATAT,² P. CHALLIS,¹ M. HICKEN,¹ R. P. KIRSHNER,¹ T. MATHESON,⁴ M. MODJAZ⁵

Accepted for publication in Ap. J.

ABSTRACT

Recent high-resolution spectra of the Type Ia SN 2006X have revealed the presence of time-variable and blueshifted Na I D features, interpreted by Patat et al. as originating in circumstellar material within the progenitor system. The variation seen in SN 2006X induces relatively large changes in the total Na I D equivalent width ($\Delta EW \sim 0.5 \text{ \AA}$ in just over two weeks), that would be detectable at lower resolutions. We have used a large data set comprising 2400 low-resolution spectra of 450 Type Ia supernovae (SNe Ia) obtained by the CfA Supernova Program to search for variable Na I D features. Out of the 31 SNe Ia (including SN 2006X) in which we could have detected similar EW variations, only one other (SN 1999cl) shows variable Na I D features, with an even larger change over a similar ~ 10 -day timescale ($\Delta EW = 1.66 \pm 0.21 \text{ \AA}$). Interestingly, both SN 1999cl and SN 2006X are the two most highly-reddened objects in our sample, raising the possibility that the variability is connected to dusty environments.

Subject headings: circumstellar matter — supernovae: general — dust, extinction

1. INTRODUCTION

Type Ia supernovae (SNe Ia) are thought to result from the thermonuclear runaway in a carbon-oxygen white dwarf (WD) star (Hoyle & Fowler 1960), having grown in mass to the Chandrasekhar critical mass (Chandrasekhar 1931). How the WD actually approaches this critical mass is still debated (e.g., Parthasarathy et al. 2007; Tutukov & Fedorova 2007), but viable hypotheses include the accretion of material from a non-degenerate binary companion (the “single-degenerate” scenario; Whelan & Iben 1973), or a merger process involving another white dwarf star (the “double-degenerate” scenario; Iben & Tutukov 1984; Webbink 1984).

While there is no direct empirical evidence for either scenario, observations suggest the existence of multiple progenitor channels. For instance, the distribution of SN Ia peak luminosities is different in early-type and late-type galaxies (the most luminous SNe Ia are found only in late-type galaxies; e.g., Hamuy et al. 2000; Jha et al. 2007). Several studies have modeled the SN Ia rate with two components: one proportional to the star formation rate, the other proportional to the total stellar mass (Mannucci et al. 2005; Scannapieco & Bildsten 2005; Sullivan et al. 2006). The dependence on the star formation rate is evidence that at least some SNe Ia originate in young stellar populations, and confirms earlier claims of an enhanced SN Ia rate in star-forming galaxies (e.g., Oemler & Tinsley 1979; van den Bergh 1990; Cappellaro et al. 1997). More recently, Pritchett et al. (2008) find that the SN Ia rate is $\sim 1\%$ of the WD for-

mation rate, independent of star-formation history, and conclude that the single-degenerate channel alone is not a viable model for all SN Ia progenitor systems (see also Yungelson & Livio 2000; Greggio 2005).

The double-degenerate scenario has been invoked as a plausible interpretation for a few unusually luminous SNe Ia (e.g., SNLS-03D3bb, Howell et al. 2006; SN 2006gz, Hicken et al. 2007). However, several hydrodynamical models suggest that double-WD mergers cause an off-center carbon ignition that leads to the conversion of C+O into O+Ne+Mg (e.g., Saio & Nomoto 2004), and subsequently to an accretion-induced collapse to a neutron star (e.g., Bravo & García-Senz 1999; although see Yoon et al. 2007). Radiation-hydrodynamics simulations of such O+Ne+Mg cores predict a weak $\lesssim 10^{50}$ erg explosion if rotation is absent, powered primarily by neutrino-energy deposition (Kitaura et al. 2006; Dessart et al. 2006). However, angular momentum is expected to be abundant in such accretion-induced collapses, resulting in a strong aspherical explosion. The predicted low ^{56}Ni yields and ejecta mass would make these events optically dim, quite unlike SN Ia explosions (Dessart et al. 2007).

A direct confirmation of the single-degenerate scenario would be the detection of circumstellar material (CSM) arising from the transfer of matter to the WD by its non-degenerate binary companion. The interaction of the SN Ia ejecta with the CSM would probably lead to detectable radio and X-ray emission, but observations at these wavelengths yield only upper limits (Panagia et al. 2006; Hughes et al. 2007). Nonetheless, strong hydrogen emission has been detected in two SNe Ia so far (SN 2002ic, Hamuy et al. 2003; SN 2005gj, Aldering et al. 2006; Prieto et al. 2007; although see Benetti et al. 2006 and Trundle et al. 2008 for a different interpretation), interpreted as evidence for ejecta-CSM interaction, and hence for a single-degenerate scenario (although see Livio & Riess 2003). However, the lack of similar detections in other SNe Ia suggests that these are rare events.

¹ Harvard-Smithsonian Center for Astrophysics, 60 Garden Street, Cambridge, MA 02138; sblondin,pchallis,mhicken,rkirshner@cfa.harvard.edu .

² European Southern Observatory, Karl-Schwarzschild-Strasse 2, D-85748 Garching, Germany; sblondin,fpatat@eso.org .

³ Dept. of Astronomy, The Ohio State University, 140 W. 18th Ave., Columbus, OH 43210; prieto@astronomy.ohio-state.edu .

⁴ National Optical Astronomy Observatory, 950 North Cherry Avenue, Tucson, AZ 85719-4933; matheson@noao.edu .

⁵ Department of Astronomy, University of California, Berkeley, CA 94720-3411; mmodjaz@astro.berkeley.edu .

Moreover, models suggest that a significant amount of material is stripped from the companion's envelope during the explosion (Chugai 1986; Livne et al. 1992; Marietta et al. 2000; Meng et al. 2007), which should lead to an observable signature in the form of a narrow $H\alpha$ emission line in the nebular spectra. No such signature has yet been detected (Mattila et al. 2005; Leonard 2007). A recent hydrodynamical investigation of the interaction between the ejecta of a Type Ia supernova and a main sequence binary companion (Pakmor et al. 2008) finds that the theoretical predictions for the mass of stripped hydrogen are consistent with the observational limits.

In a recent study, Patat et al. (2007b) reported on the possible detection of circumstellar material in the normal Type Ia SN 2006X. Using high-resolution spectra at four epochs out to ~ 2 months past explosion, they observed a complex evolution in blueshifted absorption features associated with the NaID doublet. Because of the lack of similar evolution in the Ca II H&K doublet, they concluded that the time evolution of the NaID complex is not due to line-of-sight effects in interstellar gas. Instead, the variation was attributed to ionization changes in circumstellar material (CSM) within the progenitor system, due to radiation from the supernova. The expansion velocities of this CSM ($\sim 50 \text{ km s}^{-1}$) were compatible with wind velocities for early red-giant stars, thereby favoring a single-degenerate progenitor scenario for SN 2006X.

More recent studies of SN 2000cx and SN 2007af using similar multiepoch high-resolution data have not detected any variable NaID features. No NaID absorption is detected in SN 2000cx to the level of a few $\text{m}\text{\AA}$ (Patat et al. 2007a), setting an upper limit of $2 \times 10^{10} \text{ cm}^{-2}$ on the column density of the absorbing material. In SN 2007af, Simon et al. (2007) place an upper limit of $\sim 10 \text{ m}\text{\AA}$ on the EW of circumstellar NaID lines, corresponding to a column density of $6 \times 10^{10} \text{ cm}^{-2}$.

It is therefore still unclear whether the variability in the NaID line is a common feature amongst SNe Ia, or if SN 2006X is a unique case. Chugai (2008) argues that the structure observed by Patat et al. (2007b) cannot originate in circumstellar material, based on the expected low optical depth of NaID ($\tau < 10^{-3}$) in the spherically-symmetric wind of a typical red giant (RG) star.

With a large sample of multiepoch high-resolution spectra of SNe Ia, one could address these questions directly. However, such data require dedicated programs on 8–10m telescopes, and signal-to-noise ratio (S/N) constraints restrict this study to bright events ($m_V \lesssim 15$ at peak).

In this paper, we instead use a large database of low-resolution spectra obtained through the CfA Supernova Program to investigate changes in the NaID doublet with time. The variations in the NaID profile in SN 2006X induced changes in its equivalent width (EW) of $> 0.5 \text{ \AA}$ between -2 and $+14 \text{ d}$ from maximum light. We have a unique set of hundreds of SNe Ia whose spectra we can examine for EW variations like those seen in SN 2006X. The statistical power of such a large sample enables us to place meaningful constraints on the frequency (and nature) of variable NaID features in SNe Ia.

We show that SN 2006X is not the only supernova

with variable NaID absorption, and the nature of the variable absorption we detect leads us to think that the explanation given by Patat et al. (2007b) for SN 2006X may not apply in all cases. What's more, the absence of variable absorption in most of the SNe Ia for which we have adequate data is an important clue to the nature of SN Ia progenitors.

The paper is organized as follows. In § 2 we present the spectroscopic sample used in this study. We use a Monte Carlo simulation to estimate the systematic error in our EW measurements in § 3. The results are presented in § 4 and discussed in § 5. Conclusions follow in § 6.

2. SPECTROSCOPIC DATA

To investigate the variability of NaID features in SNe Ia we have used a large spectroscopic data set obtained through the CfA Supernova Program (P.I.: R. Kirshner). Since 1994, we have obtained ~ 2400 optical spectra of ~ 450 low-redshift ($z \lesssim 0.05$) SNe Ia with the 1.5 m Tillinghast telescope at FLWO using the FAST spectrograph (Fabricant et al. 1998). The setup used (300-line/mm grating and $3''$ slit) yields a typical FWHM resolution of $\sim 6 \text{ \AA}$ ($\sim 300 \text{ km s}^{-1}$ at NaID). Several spectra were published in studies of specific supernovae (e.g., SN 1998bu; Jha et al. 1999), while 432 spectra of 32 SNe Ia have recently been published by Matheson et al. (2008). We also have complementary multi-band optical photometry for most objects (Riess et al. 1999; Jha et al. 2006; Hicken et al. 2009). All published data are available via the CfA Supernova Archive⁶.

In SN 2006X, the bulk of the variation in the NaID EW occurs before $\sim 15 \text{ d}$ past maximum light, with a timescale of $\sim 10 \text{ d}$ (Patat et al. 2007b). In order to investigate the occurrence of similar cases in our data, we only consider objects for which we have at least one spectrum before $+10 \text{ d}$ past maximum light, and for which the spectroscopic coverage spans at least 10 d . The resulting sample comprises 1826 spectra of 168 SNe Ia.

All the spectra were obtained with the same telescope and instrument, and reduced in a consistent manner (see Matheson et al. 2008 for details). The uniformity of this data set is unique and enables an accurate estimate of systematic errors in our measurements.

3. MONTE CARLO ERROR ESTIMATION

Detecting small NaID equivalent-width variations is a challenging task with low-resolution spectra. At the resolution of the FAST spectrograph (FWHM $\approx 6 \text{ \AA}$), both D_1 (5895.92 \AA) and D_2 (5889.95 \AA) lines comprising the NaID doublet are blended together. Any variation in the strength of (weaker) blueshifted components (as observed in SN 2006X; Patat et al. 2007b) will then result in a small fractional change in the total ($D_1 + D_2$) EW of a single NaID absorption feature.

In what follows we use a Monte Carlo simulation to determine the minimum detectable EW variation as a function of resolution and signal-to-noise ratio (S/N). We use the results of this simulation to estimate the number of objects for which we would detect EW variations comparable to those seen in SN 2006X.

⁶ <http://www.cfa.harvard.edu/supernova/SNarchive.html>

TABLE 1
SIMULATION PARAMETERS

| Parameter | Range |
|--|---|
| Doppler parameter (km s ⁻¹) | $b = 10$ |
| Optical thickness of main Na ID ₂ line ^a | $-1 \leq \log \tau_0 \leq 5$ |
| Number of Na ID sub-components | $1 \leq n_{\text{sub}} \leq 5$ |
| Optical thickness of sub-components ^a | $-2 \leq \log \tau_{0,\text{sub}} \leq 0$ |
| Blueshifts of sub-components (km s ⁻¹) | $0 \leq v_{\text{sub}} \leq 100$ |
| SN age (days from <i>B</i> -band maximum) | $-15 \leq t_{\text{SN}} \leq +85$ |
| Resolution ^b (Å) | $0.1 \leq \text{FWHM} \leq 15.0$ |
| Signal-to-noise ratio (per pixel) | $1 \leq \text{S/N} \leq 200$ |

^a τ_0 is the optical thickness at line center.

^b We assume there are 4.2 pixels per FWHM.

3.1. Simulation presentation

We generate synthetic Na ID profiles consisting of one main doublet and several blueshifted sub-components. In the case of SN 2006X these were interpreted as being of interstellar and circumstellar origin, respectively (Patat et al. 2007b). The simulation parameters are summarized in Table 1 and explained below.

We start by generating the main Na ID doublet at high resolution (FWHM = 0.1 Å), assuming pure absorption and a Voigt profile shape. The width of the profile is set by the so-called Doppler parameter b , which is a measure of the thermal and turbulent motions within interstellar clouds. In all that follows we set $b = 10$ km s⁻¹ (this choice has negligible impact on our results). We parametrize the doublet according to the optical thickness of the stronger D₂ line, τ_0 . (The optical thickness of the D₁ line is simply $\tau_0/2$ by virtue of the ratio of oscillator strengths).

We then generate a random number of up to five sub-components in a similar fashion, blueshifted by up to 100 km s⁻¹ with respect to the main component. This corresponds to the velocity range of winds of early red giant or late subgiant stars (e.g., Judge & Stencel 1991), that was invoked by Patat et al. (2007b) to explain the observed blueshifts of the various Na ID sub-components observed in SN 2006X. In principle, these components could form in faster winds (e.g., from main sequence or compact helium stars), or through the interaction of remnant shells of successive novae with the wind of the donor star, in which case the blueshifts could be up to an order of magnitude larger. However, we deliberately limit our investigation to match the only observed case of SN 2006X.

The top panels of Fig. 1 shows example high-resolution synthetic line profiles. In all cases the stronger main Na ID components are identical (with $\log \tau_0 = 1$), while the strength of the three (weaker) blueshifted components increases from left to right, resulting in an increase of the total EW from ~ 1.7 to ~ 2.1 Å. Note that, in our simulation, τ_0 spans six decades (Table 1), such that we also investigate cases where the main Na ID component is weaker than the blueshifted sub-components. We further consider cases where the sub-components are at the same wavelength as the main component (“blueshift” of 0 km s⁻¹), such that the main Na ID lines vary while the blueshifted sub-components do not. This situation is particularly relevant to an example of variable Na ID we present in § 4.1.

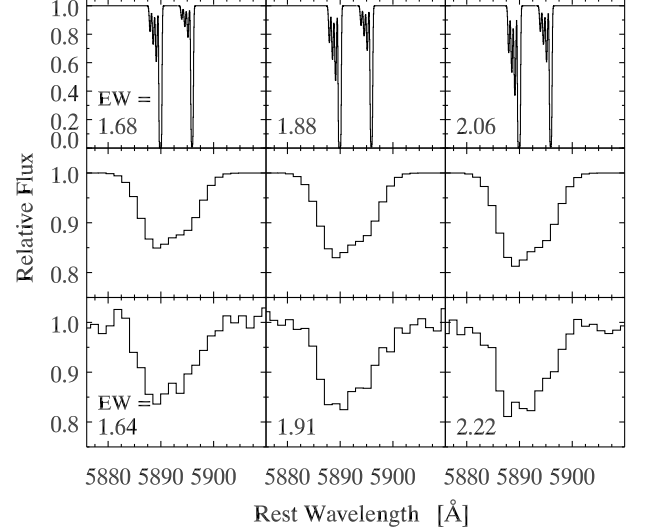


FIG. 1.— *Top*: Example input normalized line profiles, consisting of the main Na ID doublet and three weaker blueshifted sub-components. The strength of these components increases from left to right. The number in the lower-left corner is the equivalent width (in Å) of the entire profile. *Middle*: As above but at the resolution of our spectroscopic data set (FWHM ≈ 6 Å). Note the different ordinate range. *Bottom*: As above with added Poisson noise (S/N = 60 per pixel). We also report the equivalent width of the degraded profile (with a typical error ~ 0.1 Å; see § 3.2).

In measuring equivalent widths the definition of the underlying supernova pseudo-continuum is a potential source of systematic error. We account for this by multiplying the normalized Na ID profiles by SN template spectra (from Hsiao et al. 2007) at ages between -15 and $+85$ d from maximum light. The age distribution is matched to that of our data set. Over this time interval the underlying pseudo-continuum at the Na ID position changes significantly. In § 3.2 we show that this has negligible impact on the measured equivalent width.

The result is then degraded in resolution through convolution with a Gaussian profile, and resampled to 4.2 pixels per FWHM resolution to match our data. We allow for resolutions as low as 15 Å, but illustrate the typical resolution of our spectroscopic data set (FWHM ≈ 6 Å) in the middle panels of Fig. 1. While we are unable to fully resolve individual components of the Na ID doublet, the overall increase in the total EW is clearly visible.

Last, we degrade the S/N by adding Poisson noise to the lower resolution spectrum. Again, the overall increase in the total Na ID EW is visible in the bottom panels of Fig. 1.

We then measure the equivalent width as follows: we define continuum regions on either side of the D₂ and D₁ lines (or of the single Na ID line when the doublet is unresolved) spanning a maximum of 20 Å. We assume the line to span three times the width of the Doppler (Gaussian) core, or $3 \times \text{FWHM}/2\sqrt{2\ln 2} \approx 1.3 \times \text{FWHM}$, plus an additional ~ 2 Å on the blue side to account for the possible presence of blueshifted sub-components. The continuum is then determined by fitting a second-order polynomial to the continuum regions, and the equivalent width is computed over the line span defined in the usual way.

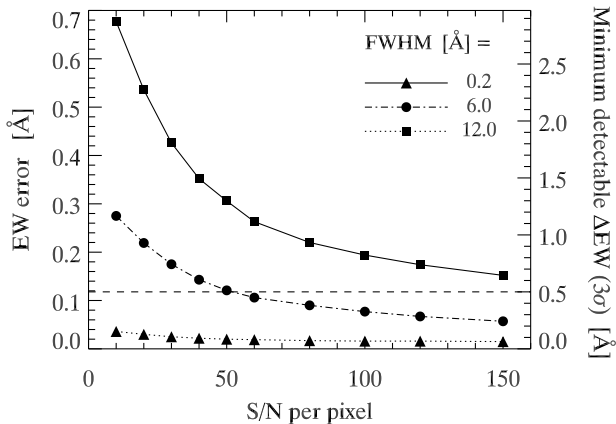


FIG. 2.— EW measurement error as a function of S/N for three FWHM resolutions. The dash-dotted curve corresponds to the resolution of our data set (FWHM ≈ 6 Å). The ordinate axis on the right indicates the corresponding 3σ error on the difference between EW measurements. The horizontal dashed line corresponds to a minimum detectable EW difference of 0.5 Å.

3.2. Simulation results

The total equivalent width measured on the synthetic profile degraded in resolution and S/N is compared with the known input total EW. We then investigate the variation of the mean and rms of the difference as a function of S/N.

We summarize the simulation results in Fig. 2 for the case where $\log \tau_0 = 1$. We show the rms residuals (or measurement error) of the difference between the true and measured total Na I D EW for three FWHM resolutions (0.2 , 6.0 , and 12.0 Å) as a function of S/N. As expected, the error decreases with increasing S/N and resolution. For a 3σ detection of an EW variation of $\gtrsim 0.5$ Å, as seen in SN 2006X between -2 and $+14$ d from maximum light (Patat et al. 2007b), the measurement error must be $\lesssim 0.1$ Å, which in turn implies $S/N \gtrsim 50$ per pixel at a FWHM resolution of 6 Å. Applying this S/N cut to our data further reduces the sample presented in § 2 to 294 spectra of 31 SNe Ia.

We find that the strength of the main Na I D component has a small systematic effect on our measurement accuracy. The mean difference between the input and measured EW is $\lesssim 0.04$ Å for $\log \tau_0 \lesssim 4$ and $S/N > 10$ per pixel (at a resolution of FWHM = 6 Å), independent of the number and strength of the blueshifted Na I D sub-components. The shape of the underlying pseudo-continuum at Na I D (which changes significantly with the age of the supernova) contributes no additional error. The measurement error due to resolution alone (i.e. the rms residuals for FWHM = 6 Å at infinite S/N) is ~ 0.01 Å. In what follows, we assume a total systematic error $\sigma_{\text{sys}} = 0.05$ Å.

4. RESULTS

Our final sample comprises SNe Ia that span a large range of known light-curve properties. In particular, the light-curve decline rate parameter $\Delta m_{15}(B)$ (Phillips 1993) ranges from 0.83 for the overluminous SN 1995al (Phillips et al. 1999) to 1.48 for the slightly underluminous SN 2005am (Folatelli & Hamuy 2008, private communication; see also Li et al. 2006). However, none of the

SNe Ia in our sample has spectra or light curves similar to the more underluminous SN 1991bg ($\Delta m_{15}(B) = 1.93$; Phillips et al. 1999).

We have measured the total Na I D EW on all 294 spectra using the same technique as for our simulated data. For each measurement, we use the corresponding error spectrum to derive the associated statistical error, which is added in quadrature to the systematic error derived from our simulation ($\sigma_{\text{sys}} = 0.05$ Å; see § 3.2).

We take special care to include only the host-galaxy Na I D line when measuring the total EW. For redshifts $cz \lesssim 800$ km s $^{-1}$, the Galactic Na I D line contributes to the host-galaxy line region defined in § 3. This affects only one SN Ia in our final sample, SN 1994D, whose host galaxy NGC 4256 is at $cz = +592$ km s $^{-1}$ (Falco et al. 1999). However, King et al. (1995) report a recession velocity of $+880$ km s $^{-1}$ at the SN position, which is the value we assume in this study. Nonetheless, the presence of Galactic high-velocity clouds inferred from high-resolution spectra (up to $+250$ km s $^{-1}$; Ho & Filippenko 1995; King et al. 1995) causes some overlap in our spectra with the Na I D absorption in NGC 4256 in the SN line of sight, and our EW measurements for SN 1994D are systematically biased towards higher values (EW = $0.32^{+0.34}_{-0.06}$ Å, cf. 0.087 ± 0.002 Å reported by Ho & Filippenko 1995 for the NGC 4256 component; see Table 2). All other 30 SNe Ia are at $cz > 800$ km s $^{-1}$, and we interpolate over any Galactic Na I D for the EW determination.

4.1. Variable Na I D in the highly-reddened SN 1999cl

The single example of variable Na I D lines observed to date, SN 2006X, is too slender a foundation on which to construct a general model for the variation. Nevertheless, we can test the null hypothesis of a constant EW against our data for each supernova. Rejecting this hypothesis constitutes detecting variability for an individual supernova.

Using a χ^2 test for a constant EW model, we find that two SNe Ia in our sample display variable Na I D features: SNe 1999cl and 2006X. While variable sodium features have already been detected in high-resolution spectra of SN 2006X (Patat et al. 2007b), their detection in our data gives us confidence in our methods and their detection in SN 1999cl constitutes a new result. The χ^2 per degree of freedom (dof) for the constant EW model is 11.23 for SN 1999cl and 4.47 for SN 2006X (Table 2). We show the EW variation for both objects in Fig. 3. All other χ^2/dof are $\lesssim 1.3$. Interestingly, both SNe 1999cl and 2006X are amongst the three most highly-reddened objects in our sample (host-galaxy reddening $E(B - V)_{\text{host}} > 1$ mag; see § 4.2). The other highly-reddened object, SN 2003cg, shows no such variation in the Na I D EW ($\chi^2/\text{dof} = 1.07$ for a constant EW model; Table 2). The EW variation for this supernova is also shown in Fig. 3. The implications of this result are discussed at length in § 5.

To our knowledge there are no (multi-epoch) high-resolution spectra of SN 1999cl to confirm our findings, but the agreement between our measurements on SN 2006X and those of Patat et al. (2007b) illustrates the accuracy of our measurements and Monte Carlo error estimation (see Fig. 3). We have further checked that

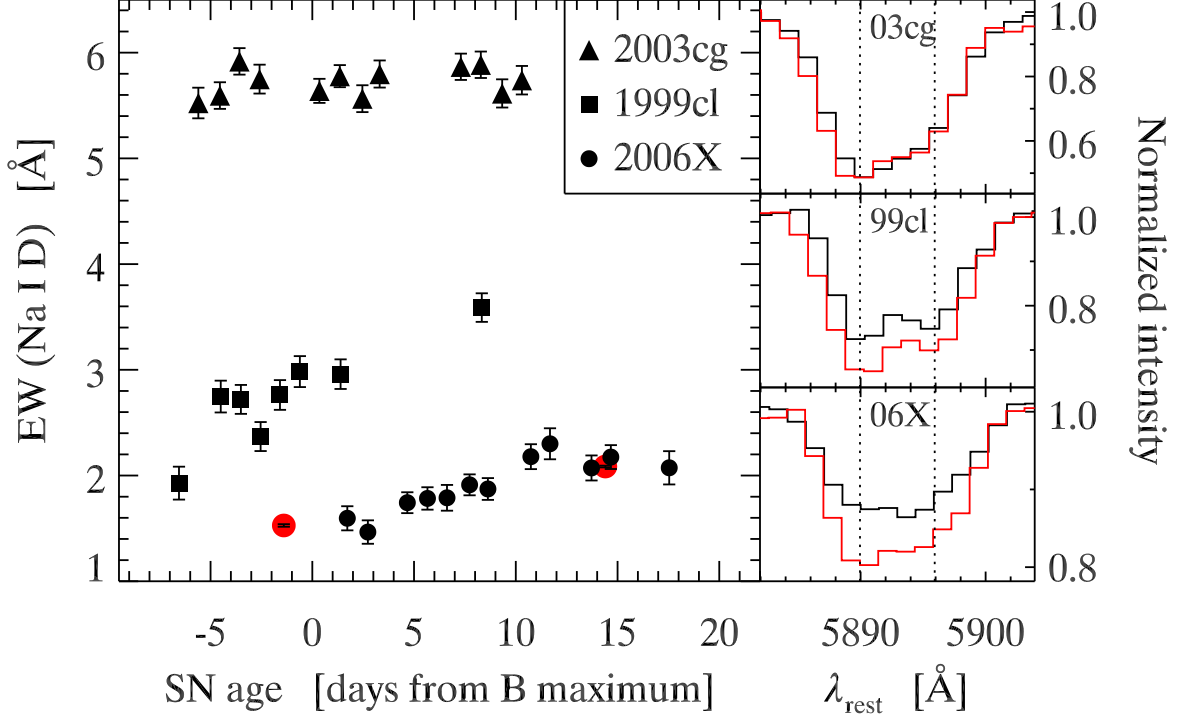


FIG. 3.— *Left*: Time-evolution of the equivalent width of the Na ID doublet for the three most highly-reddened SNe Ia in our sample: SNe 2003cg (*filled triangles*), 1999cl (*filled squares*), and 2006X (*filled circles*). Both SNe 1999cl and 2006X exhibit a variable Na ID EW, while that of SN 2003cg remains constant over time. The larger filled circles at -2 d and $+14$ d correspond to EW measurements on high-resolution (FWHM ≈ 7 km s $^{-1}$, or ~ 0.14 Å, at Na ID) VLT+UVES spectra of SN 2006X published by Patat et al. (2007b). *Right*: Normalized Na ID profiles for SN 2003cg (*top*), SN 1999cl (*middle*) and SN 2006X (*bottom*), plotted in rest-frame wavelength. The black and red lines correspond to the smallest and largest EW, respectively. Note the difference in ordinate range, decreasing from top to bottom. The vertical dotted lines indicate the wavelength positions of the individual D₁ and D₂ lines. [See the electronic version of the Journal for a color version of this figure.]

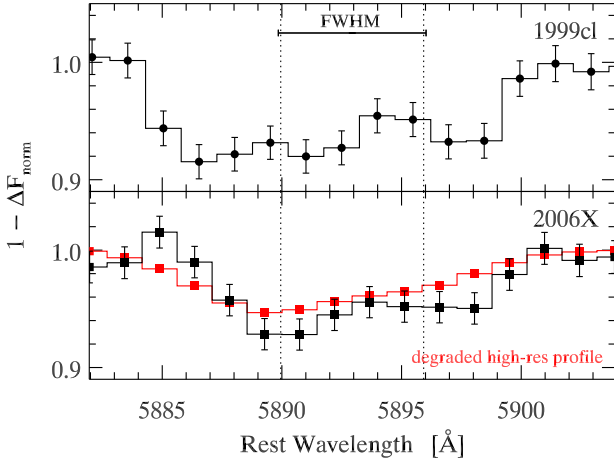


FIG. 4.— One minus the difference between the normalized Na ID profiles with the smallest and largest EW, respectively, for SN 1999cl (*top*) and SN 2006X (*bottom*). The red line in the lower panel corresponds to the variation for SN 2006X inferred by degrading the resolution of the high-resolution spectra published by Patat et al. (2007b). The vertical dotted lines indicate the wavelength positions of the individual D₁ and D₂ lines. The horizontal line in the upper panel shows the size of one the spectral resolution (FWHM ≈ 6 Å). [See the electronic version of the Journal for a color version of this figure.]

variations in seeing (and thus in spectral resolution for an object that does not fill up the $3''$ slit of the FAST spectrograph) do not correlate with the observed Na ID variations.

Note that there is a significant EW variation inferred

from high-resolution spectra at later ages in SN 2006X ($\Delta\text{EW} \approx 0.36$ Å between $+14$ and $+61$ d; Patat et al. 2007b). However, this variation is below our typical detection threshold of ~ 0.5 Å, and the data from our observations at these later ages (when the supernova is fainter) do not generally meet our S/N requirements (see § 3).

The maximum difference in the total Na ID EW is 1.66 ± 0.21 Å for SN 1999cl (i.e. 8.1σ different from zero) and 0.83 ± 0.18 Å for SN 2006X (4.5σ). Without high-resolution spectra of SN 1999cl, we cannot place useful constraints on the change in Na ID column density this would represent. We note that the EW increases with time, and that the timescale for this variation is ~ 10 d, for both objects (although this is a lower limit for SN 1999cl due to lack of suitable data). The EW variation for SN 2006X between the extrema EW values (i.e. between $+3$ d and $+12$ d past maximum) is consistent with a linear variation, with $\chi^2/\text{dof} < 1$ for a slope of ~ 0.08 Å d $^{-1}$. This is not the case for SN 1999cl, with $\chi^2/\text{dof} > 2$ for a linear fit. It is difficult to estimate the significance of the structure seen around -4 d for SN 1999cl with the available data.

We can examine more closely the Na ID profiles in Fig. 3 to study the nature of the variation seen in SN 1999cl, and in particular whether it could be different from that seen in SN 2006X. The high-resolution data for SN 2006X presented by Patat et al. (2007b) show that the variation entirely stems from weaker components blueshifted by ~ 50 km s $^{-1}$ with respect to the main saturated Na ID components. Despite the lower

TABLE 2
 REDDENING AND NaID EW MEASUREMENTS

| SN | $E(B - V)_{\text{host}}$ (mag) | EW (Å) | ΔEW (Å) | N_{σ} | χ^2/dof (const.) | dof | t_{min} (d) | Δt (d) |
|--------|-----------------------------------|------------------------|--------------------------|--------------|---------------------------------|-----|-------------------------|-------------------|
| (1) | (2) | (3) | (4) | (5) | (6) | (7) | (8) | (9) |
| 1994D | 0.04 (0.01) | $0.20^{+0.34}_{-0.06}$ | 0.40 (0.22) | 1.8 | 1.01 | 4 | -3.6 | 46.8 |
| 1994ae | 0.02 (0.01) | $0.42^{+0.11}_{-0.12}$ | 0.22 (0.11) | 2.0 | 0.87 | 9 | +1.4 | 28.8 |
| 1995al | 0.06 (0.02) | $1.13^{+0.10}_{-0.22}$ | 0.32 (0.17) | 1.9 | 0.95 | 5 | +7.0 | 13.0 |
| 1997bp | 0.19 (0.03) | $1.85^{+0.29}_{-0.23}$ | 0.52 (0.29) | 1.8 | 0.96 | 7 | -1.1 | 28.6 |
| 1997br | 0.27 (0.04) | $0.54^{+0.10}_{-0.14}$ | 0.24 (0.16) | 1.5 | 0.79 | 4 | -7.4 | 28.7 |
| 1997do | 0.10 (0.03) | $0.32^{+0.13}_{-0.10}$ | 0.23 (0.20) | 1.1 | 0.56 | 4 | -6.1 | 27.5 |
| 1997dt | 0.61 (0.07) | $1.16^{+0.27}_{-0.16}$ | 0.43 (0.30) | 1.4 | 0.89 | 4 | -9.8 | 10.8 |
| 1998aq | 0.01 (0.01) | $0.30^{+0.09}_{-0.14}$ | 0.23 (0.11) | 2.2 | 0.85 | 13 | -9.0 | 40.8 |
| 1998bu | 0.34 (0.04) | $0.27^{+0.17}_{-0.15}$ | 0.32 (0.16) | 2.0 | 1.07 | 24 | -2.7 | 59.8 |
| 1998dh | 0.17 (0.02) | $0.37^{+0.16}_{-0.12}$ | 0.28 (0.14) | 2.0 | 0.85 | 6 | -8.8 | 54.4 |
| 1998dm | 0.34 (0.05) | $0.54^{+0.18}_{-0.26}$ | 0.44 (0.27) | 1.6 | 0.81 | 5 | +5.8 | 18.9 |
| 1998es | 0.07 (0.02) | $1.58^{+0.18}_{-0.10}$ | 0.28 (0.14) | 1.9 | 0.85 | 8 | -6.0 | 30.4 |
| 1999cl | 1.20 (0.07) | $2.78^{+0.81}_{-0.85}$ | 1.66 (0.21) | 8.1 | 11.23 | 7 | -6.6 | 14.9 |
| 1999dq | 0.12 (0.03) | $1.25^{+0.23}_{-0.19}$ | 0.42 (0.20) | 2.1 | 0.68 | 12 | -8.6 | 27.6 |
| 2001V | 0.03 (0.02) | $1.34^{+0.29}_{-0.25}$ | 0.54 (0.28) | 1.9 | 0.83 | 14 | -9.3 | 33.4 |
| 2001en | 0.07 (0.04) | $1.10^{+0.21}_{-0.15}$ | 0.36 (0.18) | 2.0 | 1.24 | 6 | +2.7 | 12.6 |
| 2001ep | 0.14 (0.04) | $0.69^{+0.16}_{-0.31}$ | 0.47 (0.27) | 1.7 | 0.74 | 10 | -2.7 | 10.8 |
| 2002bo | 0.47 (0.04) | $2.64^{+0.26}_{-0.30}$ | 0.56 (0.21) | 2.6 | 1.07 | 17 | -7.0 | 28.7 |
| 2002cr | 0.09 (0.04) | $0.40^{+0.17}_{-0.16}$ | 0.33 (0.22) | 1.5 | 0.56 | 4 | -7.4 | 12.8 |
| 2002fk | 0.03 (0.02) | $0.20^{+0.06}_{-0.09}$ | 0.15 (0.09) | 1.8 | 0.75 | 5 | +3.4 | 34.6 |
| 2003cg | 1.06 (0.03) | $5.73^{+0.19}_{-0.20}$ | 0.39 (0.19) | 2.1 | 1.07 | 11 | -5.6 | 15.9 |
| 2003du | 0.01 (0.01) | $0.22^{+0.10}_{-0.07}$ | 0.17 (0.08) | 2.1 | 1.06 | 6 | +2.2 | 23.8 |
| 2003kf | 0.04 (0.03) | $0.51^{+0.20}_{-0.11}$ | 0.31 (0.16) | 1.9 | 0.92 | 11 | -6.3 | 48.5 |
| 2005am | 0.03 (0.02) | $0.23^{+0.07}_{-0.16}$ | 0.23 (0.11) | 2.1 | 1.13 | 5 | +1.4 | 11.8 |
| 2005cf | 0.10 (0.04) | $0.22^{+0.20}_{-0.08}$ | 0.28 (0.15) | 1.9 | 0.97 | 9 | -8.8 | 13.9 |
| 2006N | 0.03 (0.02) | $0.67^{+0.34}_{-0.31}$ | 0.65 (0.28) | 2.3 | 1.35 | 7 | -2.8 | 11.8 |
| 2006X | 1.47 (0.04) | $1.88^{+0.42}_{-0.42}$ | 0.83 (0.18) | 4.5 | 4.47 | 11 | +1.7 | 15.8 |
| 2007S | 0.41 (0.03) | $1.81^{+0.26}_{-0.33}$ | 0.58 (0.28) | 2.1 | 1.32 | 7 | +0.0 | 38.4 |
| 2007af | 0.14 (0.03) | $0.41^{+0.24}_{-0.17}$ | 0.41 (0.22) | 1.8 | 0.79 | 19 | -4.7 | 68.4 |
| 2007bm | 0.52 (0.04) | $2.24^{+0.20}_{-0.31}$ | 0.51 (0.22) | 2.3 | 1.21 | 6 | +1.9 | 29.8 |
| 2007ca | 0.30 (0.04) | $1.91^{+0.29}_{-0.46}$ | 0.75 (0.46) | 1.6 | 1.00 | 3 | -0.1 | 10.0 |

NOTE. — Col. (1): SN name; col. (2): host-galaxy color excess determined from fits to multi-band optical light curves using the MLCS2k2 code of Jha et al. (2007); col. (3): weighted mean EW. The upper and lower limits correspond to the maximum deviations from the weighted mean; col. (4): maximum EW difference. The 1σ error appears in between parentheses; col. (5): ΔEW divided by its 1σ error; col. (6): χ^2 per degree of freedom for a constant EW fit; col. (7): number of degrees of freedom (simply the number of data points minus one); col. (8): age (in days from B -band maximum light) of the earliest spectrum; col. (9): age range (in days) of the spectra used in the fit.

resolution of our data, the NaID profile with the largest EW (plotted in red in Fig. 3) does indeed appear skewed towards bluer wavelengths. This is more clearly visible in the lower panel of Fig. 4 where we plot one minus the difference between the NaID profiles with the smallest and largest EW (*black line*). Degrading the resolution of the high-resolution spectra of SN 2006X presented by Patat et al. (2007b) reveals a profile also skewed towards the blue (*red line*).

In contrast, the variation observed in SN 1999cl seems to affect equally all NaID components between ~ 5885 Å and ~ 5898 Å (Fig. 4; *top panel*). The largest variation is observed blueward of the NaID₁ line (around ~ 5886 Å, corresponding to a blueshift of ~ 200 km s⁻¹). However, given the low resolution of our data (FWHM ≈ 6 Å, or ~ 4 pixels), it is difficult to gauge the significance of the variation that is not centered at the rest wavelengths of

the NaID lines. Still, if all NaID components (including blueshifted ones, if present) vary by a similar amount, this would suggest the variation is associated in part with the same material where the bulk of the reddening occurs, unlike SN 2006X where the weaker variable NaID components are not associated with the material causing the large reddening towards this object (see also § 5.2).

Both SNe 1999cl and 2006X are part of the subgroup of SNe Ia with high velocity gradients in the SiII16355 absorption (HVG; see Benetti et al. 2005). A larger sample is needed to confirm the suggestion by Simon et al. (2007) that the variability is preferentially associated with the HVG subgroup. We note that our sample includes several other HVG SNe Ia (e.g., SN 2002bo) that do not display variable NaID lines.

Our measurements also show that not all blueshifted NaID components in SNe Ia are variable: Patat et al.

(2007b) noted that a high-resolution spectrum of SN 1998es around maximum light had similar Na I D line profiles as SN 2006X around the same age, but we see no evidence for variability ($EW = 1.6^{+0.18}_{-0.10}$ Å; see Table 2). Patat et al. (2007b) also noted similar profiles in the overluminous SN 1991T, but this object is not part of the sample presented in this paper.

4.2. The relation between Na I D equivalent width and host-galaxy reddening

With Na I D equivalent-width measurements for 31 SNe Ia we can independently investigate its relation with host-galaxy color excess $E(B - V)_{\text{host}}$, as has already been done by several authors using supernova spectra (Barbon et al. 1990; Richmond et al. 1994; Turatto et al. 2003). In particular, we can test whether the Na I D EW can be used to estimate the host-galaxy reddening for objects with limited photometric data.

The results are displayed in Fig. 5 and included in Table 2. Here the EW values are reported as the weighted mean of all measurements for a given supernova, while the error bars indicate the maximum deviations from the mean (this explains the large error associated with SN 1999cl, due to intrinsic variations rather than random error). The color excess in the host galaxy was determined from fits to multi-band optical light curves using the MLCS2k2 code of Jha et al. (2007), corrected for the Galactic reddening in the line-of-sight using the dust maps of Schlegel et al. (1998). Over one half of these light curves are part of a new sample that will be published soon by the CfA Supernova Group (Hicken et al. 2009).

While there is a general trend of higher color excess corresponding to higher Na I D EW (such that $E(B - V)_{\text{host}} > 0.5$ mag for $EW > 2$ Å), the scatter in $E(B - V)_{\text{host}}$ at a given EW is considerable. At $EW \approx 2$ Å for instance, $E(B - V)_{\text{host}}$ ranges from ~ 0.2 to ~ 1.5 mag. Any empirical relation based on SN Ia data can at best provide an approximate lower limit on $E(B - V)_{\text{host}}$. The points do appear to cluster around the bivariate relation of Turatto et al. (2003), albeit with a larger spread. The origin of the scatter could be due to a (global) variation in the dust-to-gas ratio in the host-galaxy interstellar medium, associated with variations in gas metallicity and dust composition (e.g., Draine et al. 2007). Effects local to the SN circumstellar environment in the form of light echoes have also been found to impact the reddening derived assuming a standard color evolution for SNe Ia (Wang 2005; Patat et al. 2006).

We note that the relation of color excess with EW is expected to be non-linear for a fixed dust-to-gas ratio because of line saturation effects at high EW, as observed by Munari & Zwitter (1997) in Galactic O and B stars. Linearity at high EW could hold if the extinction takes place in a number of clouds at different velocities, each producing unsaturated features.

5. CIRCUMSTELLAR OR INTERSTELLAR ORIGIN FOR THE VARIABLE Na I D LINES?

5.1. Conflicting interpretations of the Na I D variability

In SN 2006X, the variability of blueshifted Na I D lines was interpreted by Patat et al. (2007b) as the result of

changing ionization conditions in circumstellar material within the progenitor system due to UV radiation from the supernova. The various sub-components in Na I D then originate in the pre-SN variable wind of an early red giant companion, or from remnant shells ejected in successive nova explosions (Patat et al. 2007b). In the latter case, an asymmetric wind from the companion is needed to decelerate the material ejected during nova outbursts to match the observed $\lesssim 100$ km s $^{-1}$ blueshifts of the Na I D components. In principle, the low fraction of objects for which we detect variable Na I D lines (2/31, i.e. $\sim 6\%$) could be due to viewing angle effects (see Patat et al. 2007a).

In both SNe 1999cl and 2006X, the Na I D EW increases with age, as expected from Na II \rightarrow I recombination. The variation occurs on a similar ~ 10 d timescale, although this is a lower limit for SN 1999cl due to lack of data (see Fig. 3). At first sight, the Na I D variability seems consistent with the interpretation of Patat et al. (2007b), that it is associated with CSM in the SN Ia progenitor system.

In a recent paper, Chugai (2008) argues that the blueshifted Na I D components in SN 2006X cannot originate within CSM material from a red giant wind. The optical depth in Na I D would render it undetectable (even in high-resolution data), while that in CSM lines of Ca II H&K would be sufficient to detect them. The observed lack of variability in these calcium lines is central to the argument of Patat et al. (2007b) that the features observed in Na I D cannot be due to intervening clouds of interstellar material that are not associated with the supernova progenitor system. In contrast, Chugai (2008) use the same observational fact about Ca II to set an upper limit on the (spherically symmetric) wind from the RG companion. Unfortunately, we cannot study the variability in Ca II H&K lines with our data due to lower S/N in the blue portion of our spectra.

The variable Na I D lines observed in SN 2006X are interpreted by Chugai (2008) as being due to clusters of interstellar clouds with different calcium abundances. Whether or not this is a plausible explanation is beyond the scope of this paper, but a direct consequence of this (noted by Chugai 2008) is that the variability in Na I D should be preferentially associated with highly-reddened SNe Ia. This is certainly the case in our sample: two of the three SNe Ia with $E(B - V)_{\text{host}} > 1$ mag exhibit variable Na I D. If these time-variant features were randomly associated to all SNe Ia, independent of their reddening, the probability of finding such features only in two highly reddened Ia is very low ($\sim 0.6\%$). This fact alone is not proof that the variability is related to interstellar absorption, but is suggestive enough to warrant further scrutiny once multiepoch high-resolution spectroscopy for a larger sample is available.

5.2. The Reddening Towards SNe 1999cl and 2006X

Both SNe 1999cl and 2006X were found to be reddened by dust with unusual values of R_V , the ratio of total to selective extinction ($R_V \approx 1.6$ for SN 1999cl, Krisciunas et al. 2006; $R_V \approx 1.5$ for SN 2006X, Wang et al. 2008b), to be compared with $R_V \approx 3.1$ for the average value in the Milky-Way (e.g., Cardelli et al. 1989). Spectropolarimetry of SN 2006X has also shown that the dust producing the polarization is different from

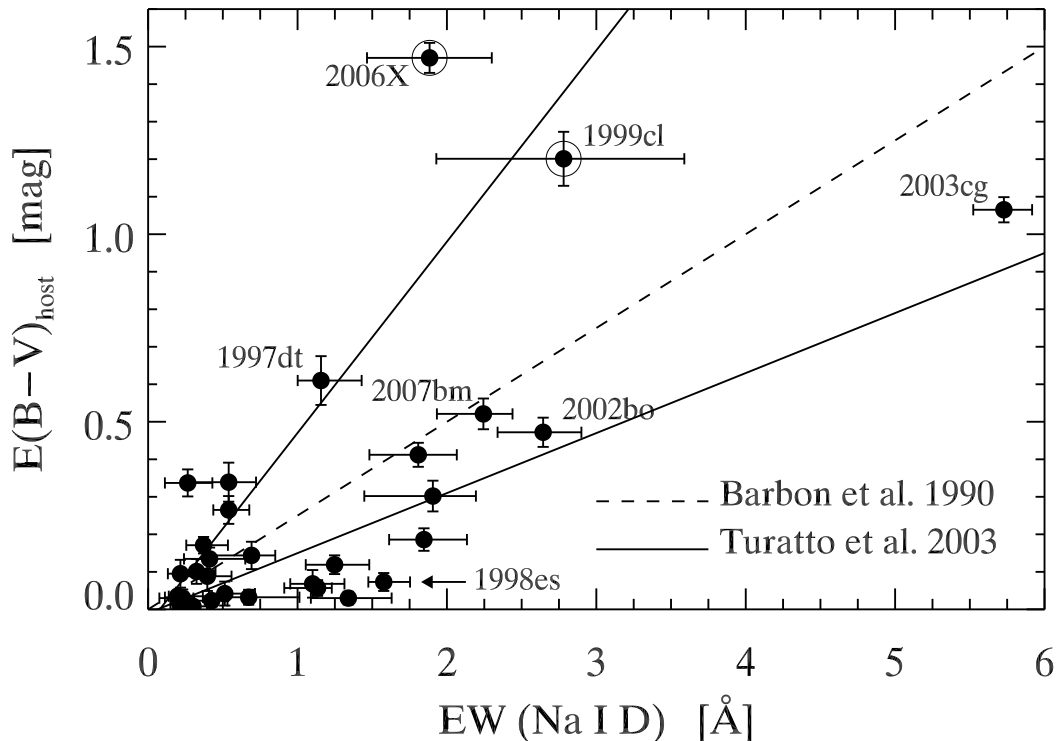


FIG. 5.— Host-galaxy color excess versus equivalent width of the Na I D doublet for the 31 SNe Ia in our sample. Also shown are the empirical relations of Barbon et al. (1990) and Turatto et al. (2003), also derived using SN Ia data.

the typical Milky Way mixture (Patat et al. 2008). Studies of larger samples also conclude that dust in the host galaxies of SNe Ia is characterized by low values of R_V (e.g., Conley et al. 2007; Hicken et al. 2009).

However, not all SNe Ia reddened by non-standard dust display variable Na I D lines: SN 2003cg has a color excess $E(B - V)_{\text{host}} \approx 1.1 \text{ mag}$ and $R_V \approx 1.8$ (Elias-Rosa et al. 2006), yet its Na I D equivalent width remains constant from one week before to two weeks past maximum light (mean $\text{EW} \approx 5.7 \pm 0.2 \text{ \AA}$; see Table 2). This suggests the variability is not systematically related to non-standard dust. If low values of R_V arise in circumstellar material around SNe Ia (see Wang 2005; Patat et al. 2006; Goobar 2008), this in turn implies that the Na I D variability does not necessarily result from effects local to the SN environment.

Patat et al. (2007b) attribute the large reddening towards SN 2006X to a dense molecular cloud, causing the strongly saturated Na I D lines and a number of weaker features (CN, CH, Ca I, diffuse interstellar bands, or DIB) at the same heliocentric velocity (Cox & Patat 2008). The column density inferred from the strongly saturated Na I D lines is $\log N(\text{Na I}) \approx 14.3$, which is two orders of magnitude larger than that of the most intense time-variant features ($\log N \approx 12$; Patat et al. 2007b). In this picture, the reddening produced by the material where these variable features arise, if any, is negligible. Additional evidence comes from the detection of a light echo associated with SN 2006X (Wang et al. 2008a; Crots & Yourdon 2008). Crots & Yourdon (2008) present compelling evidence that this echo is generated in a dust sheet $\sim 26 \text{ pc}$ in front of the supernova, presumably where the bulk of the reddening occurs, and hence is not associated with

circumstellar material.

In SN 1999cl, the variation appears to affect all Na I D components, including some with blueshifts of up to $\sim 200 \text{ km s}^{-1}$ (see Fig. 4), although the presence of such blueshifted components is difficult to confirm given the low resolution of our spectra (1 pixel corresponds to $\sim 75 \text{ km s}^{-1}$ at Na I D). We also note that we detect the DIB at $\sim 6284 \text{ \AA}$ in our low-resolution spectra of SN 1999cl at the same velocity as the Na I D absorption (the spectra of SN 1999cl have been published by Matheson et al. 2008 and are publicly available at the CfA Supernova Archive). However, this feature is too weak ($\text{EW} \lesssim 0.5 \text{ \AA}$) for us to confidently detect any variability.

The fact that we detect variable Na I D features only in the two most highly-reddened SNe Ia in our sample does suggest that the variability is somehow connected to dusty environments, and is not necessarily due to circumstellar absorption.

5.3. Variable Interstellar Lines in Galactic Stars, GRBs, and the Type II in SN 1998S

Time-variable interstellar absorption lines have been detected in high-resolution spectra of Galactic stars (see Crawford 2003 and references therein). However, the EW variation is typically $\lesssim 0.01 \text{ \AA}$ and occurs on the timescale of years to decades (cf. $\sim 1 \text{ \AA}$ over $\sim 10 \text{ d}$ for SNe 1999cl and 2006X). Another important difference is that the variation occurs in several interstellar lines (e.g., both Na I and Ca II; Crawford et al. 2002), as opposed to Na I D only (as observed by Patat et al. 2007b in SN 2006X). In most cases, the variation is associated with interstellar shells and bubbles (e.g., 7 of the 13 variable interstellar sight lines compiled by Crawford 2003

are associated with the Vela SNR). The timescale of the variation for these stars implies the existence of structure in the ISM on scales of 10–100 AU (e.g., Lauroesch et al. 2000).

Time-variable interstellar lines have also been observed in other extragalactic objects. Hao et al. (2007) report on the detection of variable Fe II and Mg II lines in low-resolution spectra of GRB 060206 (although see Thöne et al. 2008), which they interpret as stemming from interstellar patches of Mg II clouds of size comparable to the GRB beam size ($\sim 10^{16}$ cm). D’Elia et al. (2008) have revealed variable lines of Fe II in high-resolution spectra of GRB 080319B, whose fine structure was excited through pumping by the GRB UV photons. The distance to the absorbing material is constrained to be ~ 18 – 34 kpc away. (Note that the UV flux of a GRB is orders of magnitude larger than that of a SN Ia, whose ionizing/exciting capabilities are rather limited in space). In both cases the variation occurs over very short timescales (a few hours).

As noted by Patat et al. (2007b), the only other supernova with variable (and blueshifted) Na ID lines is the (core-collapse) Type II In SN 1998S (Bowen et al. 2000). In this object, however, the presence of narrow P-Cygni profiles of H and He at the same velocity as the variable Na ID lines is interpreted as the signature of outflows from the supergiant progenitor, hence associating the variability with changes in the CSM (Bowen et al. 2000; Fassia et al. 2001; see also Fransson et al. 2005).

6. CONCLUSION

We detect variable Na ID lines in low-resolution spectra of 2/31 ($\sim 6\%$) SNe Ia: SNe 1999cl and 2006X. The S/N of our spectroscopic data set is sufficiently high ($S/N > 50$ per pixel) that we can reliably detect changes of $\gtrsim 0.5$ Å in the Na ID equivalent width. This is comparable to the total EW variation seen in SN 2006X between -2 and $+14$ d past maximum light (Patat et al. 2007b). We conclude that either variable Na ID features are not a common property of SNe Ia, or that the level of the variation is less on average than observed in SN 2006X.

The limitations of this study due to the low resolution of our spectra are overcome in part by the larger statistical power of our sample.

Only a small fraction ($\sim 6\%$ in our sample) of SNe Ia display variable Na ID lines. The two SNe Ia for which

we detect variable Na ID (SNe 1999cl and 2006X) are the two most highly reddened objects in our sample, suggesting that the variability could be associated with interstellar absorption. However, we detect no such variability in the other highly-reddened SN 2003cg. We cannot exclude with our data the possibility that a larger fraction of objects display EW variations below our detection threshold of ~ 0.5 Å.

Whether the material causing the large Na ID EW variations is connected to the SN Ia progenitor system ought to become clear from multipepoch high-resolution spectroscopy for a larger sample. The detection of such variable Na ID features in an unreddened SN Ia would reduce the probability that the variability results from a purely geometrical effect in clouds of interstellar material. If variable Na ID lines remain a rare property amongst SNe Ia, this would either indicate that the variability is not associated with circumstellar material (and hence to the SN Ia progenitor system), or that there is a preferred CSM geometry for detecting the variability. It is premature with the current available data to place firm constraints on the nature of Type Ia supernova progenitor systems based on the presence or absence of variable Na ID lines alone.

It is a pleasure to thank all observers on the FLWO 1.5 m telescope, and in particular Perry Berlind and Mike Calkins, for their continued support and dedication in obtaining data for the CfA Supernova Program. We further thank Gastón Folatelli and Mario Hamuy of the Carnegie Supernova Project for communicating their $\Delta m_{15}(B)$ value for SN 2005am ahead of publication. Similar thanks go to Weidong Li for sharing the results of his MLCS2k2 fit to SN 2005am. We also acknowledge useful discussions with Joe Liske, Josh Simon, Xiaofeng Wang, and David Weinberg. MM acknowledges support from a Miller Institute Research Fellowship during the time in which part of this work was completed. We are grateful to the anonymous referee for prompting us to investigate possible differences in the nature of the Na ID variability seen in SN 1999cl and SN 2006X. Support for supernova research at Harvard University, including the CfA Supernova Archive, is provided in part by NSF grant AST 06-06772.

Facilities: FLWO:1.5m (FAST)

REFERENCES

- Aldering, G., et al. 2006, *ApJ*, 650, 510
 Barbon, R., Benetti, S., Rosino, L., Cappellaro, E., & Turatto, M. 1990, *A&A*, 237, 79
 Benetti, S., et al. 2005, *ApJ*, 623, 1011
 Benetti, S., Cappellaro, E., Turatto, M., Taubenberger, S., Harutyunyan, A., & Valenti, S. 2006, *ApJ*, 653, L129
 Bowen, D. V., Roth, K. C., Meyer, D. M., & Blades, J. C. 2000, *ApJ*, 536, 225
 Bravo, E. & García-Senz, D. 1999, *MNRAS*, 307, 984
 Cappellaro, E., Turatto, M., Tsvetkov, D. Y., Bartunov, O. S., Pollas, C., Evans, R., & Hamuy, M. 1997, *A&A*, 322, 431
 Cardelli, J. A., Clayton, G. C., & Mathis, J. S. 1989, *ApJ*, 345, 245
 Chandrasekhar, S. 1931, *ApJ*, 74, 81
 Chugai, N. N. 1986, *Soviet Astronomy*, 30, 563
 —. 2008, *Astronomy Letters*, 34, 389
 Conley, A., Carlberg, R. G., Guy, J., Howell, D. A., Jha, S., Riess, A. G., & Sullivan, M. 2007, *ApJ*, 664, L13
 Cox, N. L. J. & Patat, F. 2008, *A&A*, 485, L9
 Crawford, I. A. 2003, *Ap&SS*, 285, 661
 Crawford, I. A., Lallement, R., Price, R. J., Sfeir, D. M., Wakker, B. P., & Welsh, B. Y. 2002, *MNRAS*, 337, 720
 Crotts, A. P. S. & Yourdon, D. 2008, *ApJ*, 689, 1186
 D’Elia, V., et al. 2008, *ArXiv e-prints*, 0804.2141
 Dessart, L., Burrows, A., Livne, E., & Ott, C. D. 2007, *ApJ*, 669, 585
 Dessart, L., Burrows, A., Ott, C. D., Livne, E., Yoon, S.-C., & Langer, N. 2006, *ApJ*, 644, 1063
 Draine, B. T., et al. 2007, *ApJ*, 663, 866
 Elias-Rosa, N., et al. 2006, *MNRAS*, 369, 1880
 Fabricant, D., Cheimets, P., Caldwell, N., & Geary, J. 1998, *PASP*, 110, 79
 Falco, E. E., et al. 1999, *PASP*, 111, 438
 Fassia, A., et al. 2001, *MNRAS*, 325, 907
 Fransson, C., et al. 2005, *ApJ*, 622, 991
 Goobar, A. 2008, *ApJ*, 686, L103
 Greggio, L. 2005, *A&A*, 441, 1055
 Hamuy, M., et al. 2003, *Nature*, 424, 651

- Hamuy, M., Trager, S. C., Pinto, P. A., Phillips, M. M., Schommer, R. A., Ivanov, V., & Suntzeff, N. B. 2000, *AJ*, 120, 1479
- Hao, H., et al. 2007, *ApJ*, 659, L99
- Hicken, M., et al. 2009, *ArXiv e-prints*, 0901.4787
- Hicken, M., Garnavich, P. M., Prieto, J. L., Blondin, S., DePoy, D. L., Kirshner, R. P., & Parrent, J. 2007, *ApJ*, 669, L17
- Ho, L. C. & Filippenko, A. V. 1995, *ApJ*, 444, 165
- Howell, D. A., et al. 2006, *Nature*, 443, 308
- Hoyle, F. & Fowler, W. A. 1960, *ApJ*, 132, 565
- Hsiao, E. Y., Conley, A., Howell, D. A., Sullivan, M., Pritchett, C. J., Carlberg, R. G., Nugent, P. E., & Phillips, M. M. 2007, *ApJ*, 663, 1187
- Hughes, J. P., Chugai, N., Chevalier, R., Lundqvist, P., & Schlegel, E. 2007, *ApJ*, 670, 1260
- Iben, Jr., I. & Tutukov, A. V. 1984, *ApJS*, 54, 335
- Jha, S., et al. 1999, *ApJS*, 125, 73
- Jha, S., et al. 2006, *AJ*, 131, 527
- Jha, S., Riess, A. G., & Kirshner, R. P. 2007, *ApJ*, 659, 122
- Judge, P. G. & Stencel, R. E. 1991, *ApJ*, 371, 357
- King, D. L., Vladilo, G., Lipman, K., de Boer, K. S., Centurion, M., Moritz, P., & Walton, N. A. 1995, *A&A*, 300, 881
- Kitaura, F. S., Janka, H.-T., & Hillebrandt, W. 2006, *A&A*, 450, 345
- Kriszianas, K., Prieto, J. L., Garnavich, P. M., Riley, J.-L. G., Rest, A., Stubbs, C., & McMillan, R. 2006, *AJ*, 131, 1639
- Lauroesch, J. T., Meyer, D. M., & Blades, J. C. 2000, *ApJ*, 543, L43
- Leonard, D. C. 2007, *ApJ*, 670, 1275
- Li, W., Jha, S., Filippenko, A. V., Bloom, J. S., Pooley, D., Foley, R. J., & Perley, D. A. 2006, *PASP*, 118, 37
- Livio, M. & Riess, A. G. 2003, *ApJ*, 594, L93
- Livne, E., Tuchman, Y., & Wheeler, J. C. 1992, *ApJ*, 399, 665
- Mannucci, F., Della Valle, M., Panagia, N., Cappellaro, E., Cresci, G., Maiolino, R., Petrosian, A., & Turatto, M. 2005, *A&A*, 433, 807
- Marietta, E., Burrows, A., & Fryxell, B. 2000, *ApJS*, 128, 615
- Matheson, T., et al. 2008, *AJ*, 135, 1598
- Mattila, S., Lundqvist, P., Sollerman, J., Kozma, C., Baron, E., Fransson, C., Leibundgut, B., & Nomoto, K. 2005, *A&A*, 443, 649
- Meng, X., Chen, X., & Han, Z. 2007, *PASJ*, 59, 835
- Munari, U. & Zwitter, T. 1997, *A&A*, 318, 269
- Oemler, Jr., A. & Tinsley, B. M. 1979, *AJ*, 84, 985
- Pakmor, R., Röpke, F. K., Weiss, A., & Hillebrandt, W. 2008, *A&A*, 489, 943
- Panagia, N., Van Dyk, S. D., Weiler, K. W., Sramek, R. A., Stockdale, C. J., & Murata, K. P. 2006, *ApJ*, 646, 369
- Parthasarathy, M., Branch, D., Jeffery, D. J., & Baron, E. 2007, *New Astronomy Review*, 51, 524
- Patat, F., Baade, D., Hoefflich, P., Maund, J., Wang, L., & Wheeler, J. C. 2008, submitted to *A&A*
- Patat, F., Benetti, S., Cappellaro, E., & Turatto, M. 2006, *MNRAS*, 369, 1949
- Patat, F., et al. 2007a, *A&A*, 474, 931
- Patat, F., et al. 2007b, *Science*, 317, 924
- Phillips, M. M. 1993, *ApJ*, 413, L105
- Phillips, M. M., Lira, P., Suntzeff, N. B., Schommer, R. A., Hamuy, M., & Maza, J. 1999, *AJ*, 118, 1766
- Prieto, J. L., et al. 2007, *ArXiv e-prints*, 0706.4088
- Pritchett, C. J., Howell, D. A., & Sullivan, M. 2008, *ApJ*, 683, L25
- Richmond, M. W., Treffers, R. R., Filippenko, A. V., Paik, Y., Leibundgut, B., Schulman, E., & Cox, C. V. 1994, *AJ*, 107, 1022
- Riess, A. G., et al. 1999, *AJ*, 117, 707
- Saio, H. & Nomoto, K. 2004, *ApJ*, 615, 444
- Scannapieco, E. & Bildsten, L. 2005, *ApJ*, 629, L85
- Schlegel, D. J., Finkbeiner, D. P., & Davis, M. 1998, *ApJ*, 500, 525
- Simon, J. D., et al. 2007, *ApJ*, 671, L25
- Sullivan, M., et al. 2006, *ApJ*, 648, 868
- Thöne, C. C., et al. 2008, *A&A*, 489, 37
- Trundle, C., Kotak, R., Vink, J. S., & Meikle, W. P. S. 2008, *A&A*, 483, L47
- Turatto, M., Benetti, S., & Cappellaro, E. 2003, in *From Twilight to Highlight: The Physics of Supernovae*, ed. W. Hillebrandt & B. Leibundgut, 200–+
- Tutukov, A. V. & Fedorova, A. V. 2007, *Astronomy Reports*, 51, 291
- van den Bergh, S. 1990, *PASP*, 102, 1318
- Wang, L. 2005, *ApJ*, 635, L33
- Wang, X., Li, W., Filippenko, A. V., Foley, R. J., Smith, N., & Wang, L. 2008a, *ApJ*, 677, 1060
- Wang, X., et al. 2008b, *ApJ*, 675, 626
- Webbink, R. F. 1984, *ApJ*, 277, 355
- Whelan, J. & Iben, I. J. 1973, *ApJ*, 186, 1007
- Yoon, S.-C., Podsiadlowski, P., & Rosswog, S. 2007, *MNRAS*, 380, 933
- Yungelson, L. R. & Livio, M. 2000, *ApJ*, 528, 108